PROCEEDINGS, TOUGH Symposium 2003
Lawrence Berkeley National Laboratory, Berkeley, California, May 12–14, 2003

ESTIMATING LARGE-SCALE FRACTURED ROCK PROPERTIES FROM RADON DATA COLLECTED IN A VENTILATED TUNNEL

André Unger, Stefan Finsterle, and Gudmundur S. Bodvarsson

Lawrence Berkeley National Laboratory
Earth Sciences Division, Mail Stop 90-1116
Berkeley, CA 94720
e-mail: AJAUnger@lbl.gov

ABSTRACT

To address regulatory issues regarding worker safety, radon gas concentrations have been monitored as part of the operation of a deep tunnel excavated from a highly fractured tuff formation. The objective of this study was to examine the potential use of the radon data to estimate large-scale formation properties of fractured rock. An iTOUGH2 model was developed to predict radon concentrations for prescribed ventilation rates. The numerical model was used (1) to estimate the permeability and porosity of the fractured formation at the length scale of the tunnel and extending tens of meters into the surrounding rock, and (2) to understand the mechanism leading to radon concentrations that potentially exceed the regulatory limit. The mechanism controlling radon concentrations in the tunnel is a function of atmospheric barometric fluctuations propagated down the tunnel. In addition, a slight suction is induced by the ventilation system. The pressure fluctuations are dampened in the fractured formation according to its permeability and porosity. Consequently, as the barometric pressure in the tunnel drops, formation gases from the rock are pulled into the opening, resulting in high radon concentrations. Model calibration to both radon concentration data measured in the tunnel and gas–phase pressure fluctuations observed in the formation yielded independent estimates of effective, large-scale fracture permeability and porosity. The calibrated model was then used as a design tool to predict the effect of adjusting the ventilation-system operation strategy for reducing the probability that radon gas concentrations will exceed the regulatory limit.

INTRODUCTION

This study examines the potential use of radon concentration data to estimate large-scale formation properties of fractured formations. Radon concentrations were measured in a large diameter tunnel, ventilated by drawing atmospheric air and formation gases containing high levels of radon into the tunnel. We then developed an iTOUGH2 (Finsterle, 1999a,b,c) model based on a review of available radon concentration data, gas-phase pressure measurements within the tunnel and the adjacent formation, and airflow rates caused by ventilation. The numerical model was then calibrated against the radon concentration and pressure data to estimate the large-scale permeability and porosity of the fractured rock. The model was subsequently used to investigate the mechanism leading to radon concentrations in excess of 1,110 Bq/m^3 (30 pCi/L), which is the current 10 CFR Part 20 (NRC, 1999) derived air concentration limit for radon.

According to 10 CFR 20 (NRC, 1999), derived air concentration (DAC) means "the concentration of a given radionuclide in air which, if breathed by the reference man for a working year of 2,000 hours under conditions of light work (inhalation rate 1.2 cubic meters of air per hour), results in an intake of one ALI [annual limit on intake]." An ALI "means the derived limit for the amount of radioactive material taken into the body of an adult worker by inhalation or ingestion in a year. ALI is the smaller value of intake of a given radionuclide in a year by the reference man that would result in a committed effective dose equivalent of 5 rems (0.05 Sv) or a committed dose equivalent of 50 rems (0.5 Sv) to any individual organ or tissue" (NRC, 1999).

CONCEPTUAL MODEL

The conceptual model of the combined rock/tunnel system is based on the recognition that atmospheric barometric-pressure fluctuations and radon concentrations propagate down the tunnel as air flows under reduced pressure (relative to the atmosphere) towards the ventilation exhaust fan. The amplitude of these barometric pressure fluctuations is dampened as air flows into and out of the fractured formation. For instance, a drop in barometric pressure within the tunnel causes formation gases to flow into the opening and mix with the ventilated air. Given that the ambient gas within the formation contains radon, concentrations within the tunnel will increase along the direction of ventilation. Differences between radon concentrations measured at two points along the tunnel contain information about the formation's permeability and porosity.

Radon concentration data (Figure 1) were collected over a period of 20 days in the ventilated tunnel, at two stations approximately 1,550 m apart. The ambient radon concentration within the formation is

estimated to be ~100,000 Bq/m^3. As formation gas enters the tunnel and mixes with ventilated air, this high radon concentration is quickly diluted to a maximum value of 2,204 Bq/m^3. However, despite the considerable dilution, radon concentration levels still frequently exceed 1,110 Bq/m^3 over the 20-day period shown in Figure 1. Note that being exposed to 1,110 Bq/m^3 for a relatively short time period does not necessarily violate the safety standard put forth by 10 CFR 20 (NRC, 1999), as long as the DAC does not exceed that limit. The arithmetic mean concentration at the upstream and downstream ends over the 20 day period shown on Figure 1 (which we assume is analogous to the DAC) is 443 Bq/m^3 and 693 Bq/m^3, respectively.

Pressure fluctuations were monitored at the land surface, in the tunnel, and within the formation approximately 18 m from the tunnel. As shown in Figure 2, the pressures in the tunnel closely track the surface signal (shifted by a constant value because of the lower tunnel elevation). Fluctuations in the rock, however, exhibit a smaller amplitude and a slight shift in time, caused by the dampening effect of the formation. This offset creates a pressure gradient and thus the driving force for gas exchange between the tunnel and the formation.

An additional data set needed for the modeling is the air velocity in the tunnel caused by the ventilation regime. As shown in Figure 3, the air velocity in the tunnel changes stepwise depending on the number of exhaust fans in operation. The mean ventilation rate was estimated as 91 m^3/s, affecting the dilution capacity of the atmosphere in the tunnel.

There appears to be a distinct correlation between the radon peaks and the time when ventilation was increased. Increasing ventilation also results in increased suction, drawing a pulse of formation gases into the tunnel. This effect is captured by the pressure data, which are prescribed as a time-varying boundary condition.

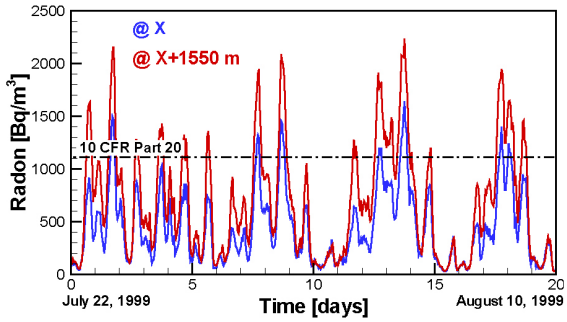

Figure 1. Radon concentrations in ventilated tunnel measured at two locations 1550 m apart. Downwind concentrations are higher because of influx of formation gas.

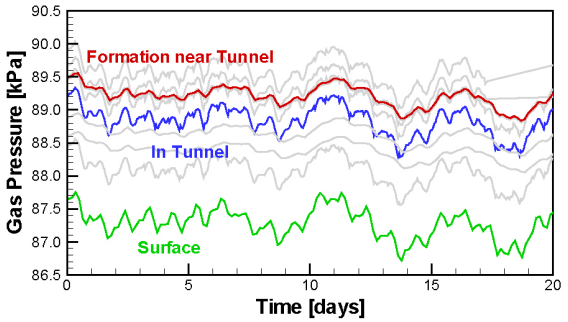

Figure 2. Gas pressure data measured at the land surface, in the tunnel, and in the formation near the tunnel

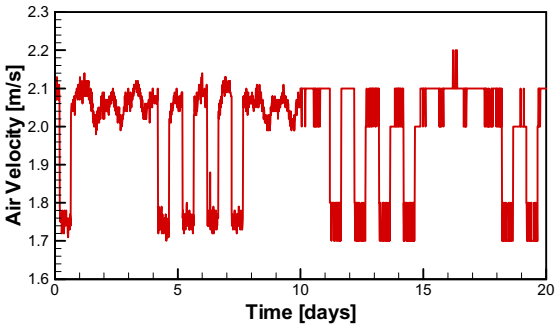

Figure 3. Air velocity in the ventilated tunnel

NUMERICAL MODEL

A numerical model was developed using iTOUGH2 in combination with the flow and transport module EOS7r (Pruess, 1991; Oldenburg and Pruess, 1995). The physical processes relevant to the conceptual and numerical model presented here involve a two-phase gas-liquid system in which the water is immobile (at residual saturation) while the gas phase is mobile. The three components considered are air, water, and radon (^{222}Rn). All three components can partition into the two phases. Given that the gas phase is the only mobile phase, advection of the three components only occurs in the gas phase. As radon is transported within the tunnel and the fractured formation, it decays with a half-life of 3.823 days.

We developed a cylindrical model, with the length axis oriented along the tunnel and the radial axis from the center of the tunnel into the formation. The model simulates a tunnel of 1,549 m in length. The outer radius of the model was assigned a distance of 66.45 m, where a pressure sensor indicates that barometric-pressure fluctuations are no longer influenced by the tunnel.

Figure 4 shows the mesh used in the numerical model, which consists of 3 nodes along the length axis (used to represent air flow down the tunnel) and 50 nodes along the radial axis of the model (used to resolve gas-phase flow and radon transport in the formation and into the tunnel).

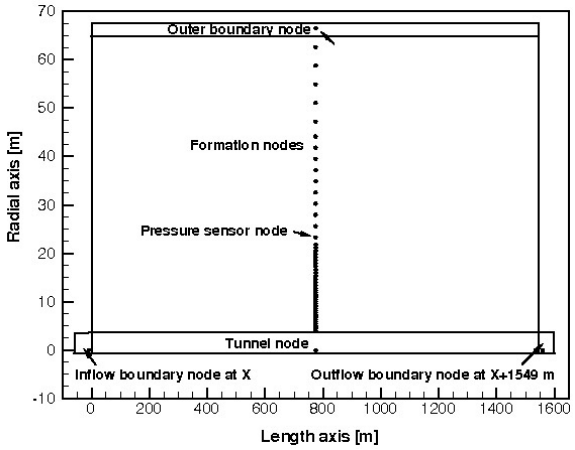

Figure 4. Plan view of mesh used in the numerical model. Dots represent the centroids of the gridblocks.

This model is essentially one-dimensional, involving transient radial flow of air and transport of radon in the formation, as well as uniform mixing of the formation gas with the air in the ventilated tunnel. The geometric simplification of the model was based upon the observation that the rate of ventilated air flushes the entire volume between X and X + 1,549 m every twenty minutes, whereas the wavelength of the radon peaks shown in Figure 1 are on the order of half a day. With this in mind, we conceptualized the tunnel as a simple mixing volume rather than a long tube requiring multiple nodes to discretize and resolve flow and transport along its length. The accuracy of this assumption was verified by calculating radon concentrations at X + 1,549 m, using a variation of the model in which the tunnel was discretized into 100 nodes. Both the low- and high-resolution models yielded identical results, with the computational burden of the latter being orders of magnitude greater.

Nodes comprising the formation represented a single fracture continuum with a low water saturation of 0.05, which is considered immobile. Liquid water has been introduced only to obtain vapor saturated conditions in the gas phase. Nodes comprising the tunnel were assigned an artificially high permeability of 1×10^{-2} m^2 to limit pressure loss along the tunnel, while maintaining smooth convergence of the Newton iteration within TOUGH2.

Time-dependent gas pressures were specified along the radial perimeter of the model (outer boundary node); the constant radon concentration along the perimeter will be estimated as one of the adjustable parameters. Air was injected in the tunnel inflow boundary node at a predefined ventilation rate. The radon concentration of the injected gas phase followed the blue signal shown in Figure 1. At the outflow boundary node, time-varying gas pressures were specified, following the barometric fluctuations shown measured in the tunnel (see Figure 2).

MODEL CALIBRATION

Calibration of the numerical model was performed using iTOUGH2 (Finsterle, 1999a,b,c) with the Levenberg–Marquardt algorithm. Calibration targets included the pressure data measured 18 m from the tunnel wall (see red line in Figure 2) and the radon concentration data measured in the tunnel at X + 1,549 m (red line in Figure 1). Calibration was performed against data from Day 2 (July 22, 1999) to Day 10 (July 31, 1999), whereas data from Day 10 to Day 20 (August 10, 1999) were used for testing the predictive capabilities of the calibrated model.

Six parameters controlling the behavior of the physical model were estimated by iTOUGH2. These were the permeability and porosity of the fracture continuum, the ambient radon concentration in the formation, an independent pressure shift for both the pressure at the outer boundary and the pressures 18 m from the tunnel wall, and the ventilation rate. Here, we assumed that the datum of the pressure transducer in the tunnel is known reliably well, whereas the datum for the transducers in the formation is unknown or uncertain. The pressure shift also automatically corrects these data sets for a static gravity potential, so that they are evaluated at the same elevation in the physical model of the tunnel. The ventilation rate was estimated because of the difficulty in calculating the ventilation rate based upon point measurements of air velocity. *A priori* estimates of ventilation rate were based on multiplying the air velocity data (see Figure 3) by the cross-sectional area of the tunnel, with the mean ventilation rate equal to 91 m^3/s.

Figure 5 shows the measured, calibrated, and predicted formation pressures and the radon concentrations in the tunnel. The calibrated and predicted pressure and radon signals show an accurate fit, with the greatest deviation occurring during the radon peaks. These peaks occur at the times when the greatest pressure differential occurs between the formation and the tunnel, and flow of formation gases into the tunnel is greatest.

In general, the flow of air is from the formation into the tunnel, owing to the slight pressure drop induced by the exhaust fans. The pressure drop was calculated to be on average 154 Pa. Flow reversals (i.e., flow from the tunnel into the formation) occur only after a sharp pressure increase in the tunnel. These flow reversals are of short duration and characterized by low radon concentrations in the tunnel (equal to the upstream concentration at X), which get pushed approximately 10 m into the formation. The highest radon concentration occurred at 13.75 days and was

driven by a pressure differential of 436 Pa between the pressure sensor in the rock and the tunnel. This peak was followed by a flow reversal at 15.25 days, driven by a pressure differential of only 18 Pa.

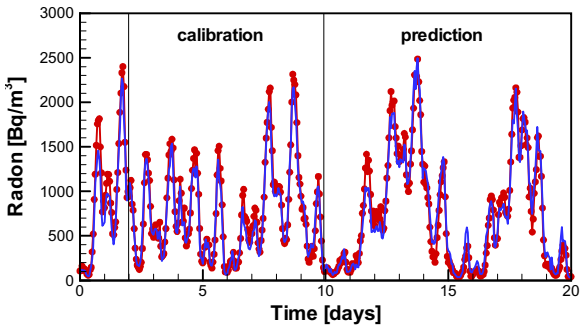

(a)

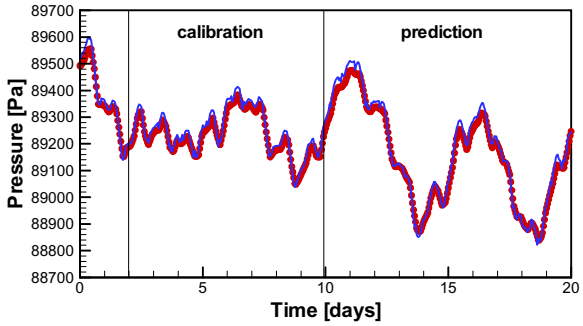

(b)

Figure 5. Comparison between measured (symbols) and calculated (line) radon concentrations and gas pressures. Only the data between Days 2 and 10 were used for calibration.

Estimated parameters and their standard deviations, as well as the matrix of direct correlations between pairs of parameters, are provided in Tables 1 and 2, respectively. Permeability and porosity are relatively strongly correlated, as expected because the gas diffusivity (which contains both parameters) affects the attenuation and phase lag of the pressure signal (Ahlers et al., 1999):

$$D_g = \frac{k\overline{P}}{\phi\mu} \tag{1}$$

Here, k is the gas permeability, $\overline{P}$ is the average gas pressure (~88 kPa), ϕ is the porosity, and μ is the gas viscosity (~1.8×10^{-5} Pa·s). The permeability, ambient radon concentration, and ventilation rate are highly correlated, suggesting that the model is over-parameterized and pointing to the possible non-uniqueness of the calibrated parameter set. This is reflected in the large standard deviations of the ambient radon concentration and ventilation rate. The strong correlation between these parameters supports the physical model representation of a relatively simple mixing problem, in which radon from the formation is diluted by the ventilated air in the tunnel. In this case, it is not reasonable to estimate the permeability of the formation, which controls the Darcy flux of the gas phase through the rock as well as the ambient radon concentration. When the Darcy flux of the gas phase and the ambient radon concentration are multiplied together, they yield the mass flux of radon into the tunnel. Independent measurement of the ambient radon concentration is required to uniquely determine permeability and porosity.

Finally, we increased the ventilation rate by a factor of 1.4 relative to the a priori mean ventilation rate. This scaling underlies the difficulty in estimating the ventilation rate from point measurements of air velocity. Ideally, this model calibration exercise should be restricted to estimating the permeability and porosity with *a priori* estimates of ambient radon concentration, the datum of the pressure transducers, and the ventilation rate known to a high degree of accuracy.

Table 1. Mean and standard deviations for the six estimated parameters in the physical model

Parameter	Estimate	Standard Deviation
$\log_{10}$(permeability [m^2])	-11.00	0.12
$\log_{10}$(porosity [-])	-3.47	0.27
Ambient radon concentration [Bq/m^3]	110,000	28,000
Pressure shift at observation sensor [Pa]	–260.0	3.3
Pressure shift at outer boundary [Pa]	346.0	5.2
Rate of ventilated air (mean value) [m^3/s]	127.0	26.5

Table 2. Matrix of direct correlations for the six estimated parameters

	Log_{10} (Perm.)	Log_{10} (Porosity)	Radon Concen.	Observation Pressure	Boundary Pressure	Ventilation Rate
Log_{10}(Permeability)	1.00	0.89	–0.99	0.00	–0.45	0.99
Log_{10} (Porosity)	0.89	1.00	0.88	–0.01	0.41	–0.89
Radon Concentration	–0.99	0.88	1.00	0.00	–0.44	0.99
Shift Observation Pressure	0.00	–0.01	0.00	1.00	–0.85	0.00
Shift Boundary Pressure	–0.45	0.41	–0.44	–0.85	1.00	0.44
Ventilation Rate	0.99	–0.89	0.99	0.00	0.44	1.00

A unique contribution from the joint inversion of the gas pressure and radon data is the relatively independent estimation of fracture permeability and porosity. This is visualized in Figure 6, which shows contours of the objective function as a function of permeability and porosity when both radon and pressure data are used for the inversion. The objective function is primarily determined from radon data residuals and is significantly less sensitive to pressure data. In particular, the minimum of the objective function indicates that the permeability estimate is well constrained (with a standard deviation of $\log_{10}$ (k [m^2]) of 0.12), whereas the standard deviation for $\log_{10}$-porosity is 0.27, i.e., only an order-of-magnitude estimate of porosity can be obtained.

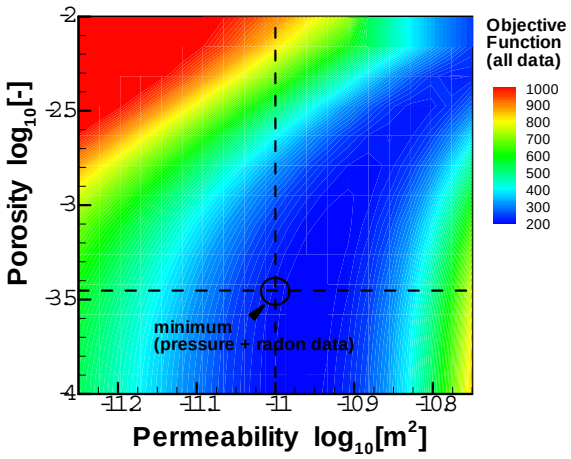

Figure 6. Contours of objective function in the parameter space spanned by $log_{10}(k\ [m^2])$ and $log_{10}(\phi)$, showing a unique minimum.

The estimated effective permeability is larger than values determined from small-scale air-injection tests performed in the same formation (Freifeld, 2001). This is a result of the large support scale of the concentration and pressure data collected in the tunnel, which tends to capture larger conductive features usually missed by smaller-scale tests such as those conducted by Freifeld (2001). Moreover, the permeability estimated from radon concentration data reflects the transport process, which may be different from the flow process reflected in pressure data. The transport of radon is expected to be preferentially channeled in the larger-aperture, kinematically connected fractures. This subset of fractures would have a higher permeability and smaller porosity relative to the total fracture network. In contrast, propagation and dampening of gas pressure fluctuations is a diffusive process that occurs in all of the connected fractures, including dead-end fractures that do not participate in radon transport. Estimates based on pressure data alone yield a lower net permeability and higher porosity.

DESIGN OF VENTIATION REGIME

In this study, we examine the ventilation regime with the goal to minimize the probability that concentrations exceed 1,110 Bq/m^3 of radon at any position within the tunnel. This could easily be achieved by overpressurizing the tunnel relative to the formation by reversing the fans, which would ensure that the tunnel contains radon-free atmospheric air. In this study, we assume that the current ventilation method of underpressurizing the tunnel will be continued.

We assume that the observed pressure fluctuations over the twenty-day period represent a stationary realization of the general, stochastic barometric signal. Then, we can interpret the difference in radon concentration levels between the two locations shown in Figure 1 as the gain in radon along a 1,549 m section of the tunnel, given a stochastic barometric-pressure signal caused by atmospheric conditions. For a given fracture permeability, porosity, ambient radon concentration, and ventilation rate, there is a probability of 0.06 that radon concentration at the inflow boundary X exceeds 1,110 Bq/m^3 over the twenty-day observation period. At the downstream end of the section (at X + 1,549 m), the probability of exceeding a level of 1,110 Bq/m^3 increases to 0.22, reflecting a gain of radon over the 1,549 m length of the tunnel.

The calibrated model was used as a ventilation-system design tool by calculating the ventilation rate needed to reduce the probability that radon concentrations will exceed 1,110 Bq/m^3 at a given position

along the tunnel. Radon concentrations were calculated at X + 1,549 m for three different ventilation rates: 127 m^3/s (which was obtained from the calibrated model), 254 m^3/s, and 64 m^3/s, with the latter two rates obtained by doubling and halving the calibrated rate, respectively. Increasing the ventilation rate enhances the pressure gradient and thus increases the absolute influx of radon. However, the dilution effect in the tunnel outweighs the increased radon influx, resulting in overall lower radon concentrations, as shown in Figure 7.

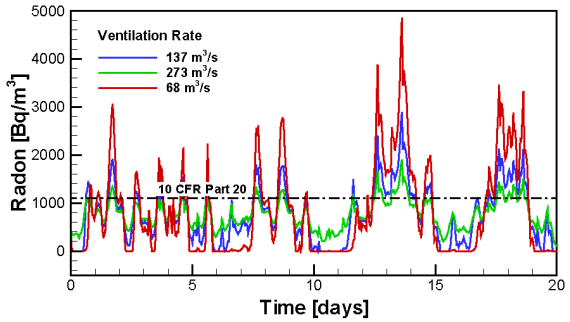

Figure 7. Predicted radon concentrations at X + 1,549 m for three different ventilation rates.

In order to calculate radon concentrations and exceedence probabilities at any point in the tunnel, we calculated the average gain in radon concentration per meter of tunnel. For this calculation, a zero radon concentration was prescribed at the inflow boundary node, representing air from outside the tunnel. Furthermore, we assumed that the pressure differential between the ambient atmospheric pressure and the formation is proportional to the ventilation rate. Finally, the simulated gain in radon concentration is divided by the 1,549 m length of the tunnel section used in the calibrated model, to yield the radon gain per meter of tunnel. Figure 8 shows the probability of exceeding a certain radon concentration level at the end of a 5 km long tunnel. Here, the exceedence probability is defined as the fractional time that radon concentrations are higher than 1,110 Bq/m^3. The probability is obtained by scaling the radon gain per meter by a factor of 5,000 and calculating the percentage of time during the twenty-day period when the radon concentration exceeded 30 pCi/L.

The exceedence probability is shown for a ventilation rate of 127 m^3/s as a function of permeability and ambient radon concentration, which are two sensitive but uncertain parameters. As is obvious from Figure 6, porosity has a limited impact on the predicted radon concentrations (and pressures). The dashed box shown in Figure 8 defines the 95% confidence interval for the estimated permeability and ambient radon concentrations. The exceedence probability increases dramatically as the permeability and ambient radon concentration deviate above the estimated values. Increased permeability or ambient radon concentration yields a larger mass flux of radon into the tunnel. This increase in the mass flux of radon then causes a corresponding increase in the exceedence probability.

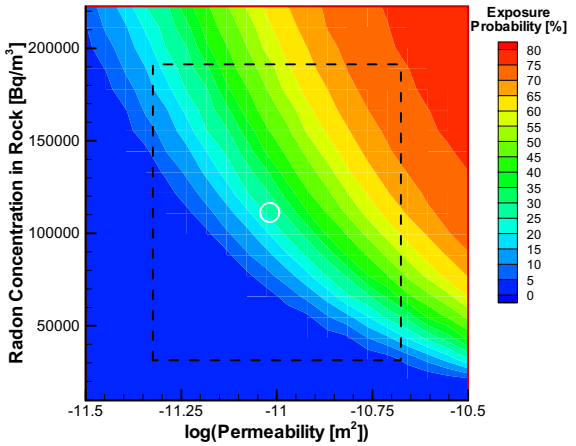

Figure 8. Probability of exceeding a radon concentration of 1,110 Bq/m^3 as a function of permeability and ambient radon concentration.

SUMMARY AND CONCLUSIONS

We developed a simple conceptual and numerical model from available radon concentration measurements in a ventilated tunnel—as well as barometric pressure fluctuations in the tunnel and within the adjacent fractured rock. Our model was based on the hypothesis that atmospheric barometric fluctuations propagate down the tunnel along with ventilation-induced air flow. The amplitudes of these barometric fluctuations are dampened as air flows through the fractured formation. A drop in barometric pressure causes formation air to flow into the tunnel, where it mixes with the ventilated air. Because ambient gas within the formation has a significantly higher radon content, gas flowing from the rock into the tunnel causes a rise in radon concentrations within the ventilated air.

Calibration of the numerical model to the available radon and pressure data confirmed the hypothesis regarding the mechanism controlling radon concentrations in the tunnel. Calibration also allowed the estimation of effective parameters representative of a large section of fractured rock. Furthermore, the radon data suggest that transport of radon is preferentially focused within the larger aperture fractures, yielding a higher permeability and lower porosity relative to values obtained from the pressure data only.

Measured and predicted radon levels within the tunnel periodically exceed a level of 1,110 Bq/m^3.

This is because the ventilation system operates under suction. The exceedence probability increases along the length of the tunnel because of the continuous influx of radon from the formation. Our calibrated model was used as a design tool to predict the effect of adjusting the ventilation rate on reducing the exceedence probability. Model results indicate that as the ventilation rate is increased from 64 m^3/s to 127 m^3/s and to 254 m^3/s, the exceedence probability at a location 5 km into the tunnel decreases from 0.30 to 0.26 and 0.12, respectively. This implies that the benefits of dilution on reducing overall radon concentrations caused by an increase in ventilation rate outweigh the increase in formation gases pulled into the tunnel (as the pressure differential between the tunnel and the formation is increased). However, the exceedence probability is very sensitive to permeability and ambient radon concentration, and increases dramatically if either of these values deviates above their estimates.

The study demonstrates the use of iTOUGH2 for (1) estimation of effective, large-scale formation properties by means of a joint inversion of different data types, and (2) extensive sensitivity and uncertainty propagation analyses to address an engineering design problem, which ultimately will be used for a health-risk evaluations.

ACKNOWLEDGMENT

The reviews of C. Oldenburg and B. Faybishenko are greatly appreciated. This work was supported by the Director, Office of Civilian Radioactive Waste Management, U.S. Department of Energy, through Memorandum Purchase Order EA9013MC5X between Bechtel SAIC Company, LLC, and the Ernest Orlando Lawrence Berkeley National Laboratory (Berkeley Lab). The support is provided to Berkeley Lab through the U.S. Department of Energy Contract No. DE-AC03-76SF00098.

REFERENCES

Ahlers, C.F., S. Finsterle, and G.S. Bodvarsson, Characterization and prediction of subsurface pneumatic response at Yucca Mountain, Nevada, *Journal of Contaminant Hydrology*, 38, 47–68, 1999.

Finsterle, S., *iTOUGH2 User's Guide*, Report LBNL-40040, Lawrence Berkeley National Laboratory, Berkeley, Calif., 1999a.

Finsterle, S., *iTOUGH2 Command Reference*, Report LBNL-40041 (rev.), Lawrence Berkeley National Laboratory, Berkeley, Calif., 1999b.

Finsterle, S., *iTOUGH2 Sample Problems*, Report LBNL-40042 (rev.), Lawrence Berkeley National Laboratory, Berkeley, Calif., 1999c.

Freifeld, B.M., *Estimation of Fracture Porosity in an Unsaturated Fractured Welded Tuff Using Gas Tracer Testing*, Ph.D. Thesis: Department of Civil and Environmental Engineering, University of California, Berkeley, Calif., 2001.

NRC (US Nuclear Regulatory Commission). *10 CFR 20. Energy: Standards for Protection against Radiation,* Washington D.C., 1999.

Oldenburg, C.M., and K. Pruess, *EOS7R: Radionuclide Transport for TOUGH2*, Report LBL–34868, Lawrence Berkeley Laboratory, Berkeley, Calif., 1995.

Pruess, K., *TOUGH2—A General–Purpose Numerical Simulator for Multiphase Fluid and Heat Flow*, Report LBL–29400, Lawrence Berkeley Laboratory, Berkeley, Calif., 1991.